Title
Relating Actual and Effective Ventilation in Determining Indoor Air Quality

Authors
Sherman, M.H.
Wilson, D.J.

Publication Date
1986-09-01

Lawrence Berkeley Laboratory
UNIVERSITY OF CALIFORNIA

APPLIED SCIENCE DIVISION

Submitted to Building and Environment

RELATING ACTUAL AND EFFECTIVE VENTILATION
IN DETERMINING INDOOR AIR QUALITY

M.H. Sherman and D.J. Wilson

September 1986

APPLIED SCIENCE
DIVISION

Prepared for the U.S. Department of Energy under Contract DE-AC03-76SF00098

DISCLAIMER

Accepted for publication in Building and Environment, August 1986.

RELATING ACTUAL AND EFFECTIVE VENTILATION IN DETERMINING INDOOR AIR QUALITY

M. H. Sherman

Energy Performance of Buildings Group
Applied Science Division
Lawrence Berkeley Laboratory
University of California
Berkeley, California, 94720

D. J. Wilson

Department of Mechanical Engineering
University of Alberta
Edmonton, Canada, T6G 2G8

ABSTRACT

Ventilation is both a mechanism for removing indoor air pollutants, and a potential energy load on the heating or cooling system of a building. Quantitative estimates of the ventilation rates, important for both of these applications, necessitate determining time-averaged quantities. The time-averaged ventilation rate appropriate for indoor air pollution, however, is different from that associated with energy load. We derive ventilation efficiencies for well-mixed, homogeneous, time-varying concentrations and corroborate findings with field data from a test house in Edmonton, Alberta, which indicate that monthly ventilation efficiency ranges from 79% to 92% with an annual average of 80%, and that hourly temporal ventilation efficiencies vary over a much larger range than time-averaged quantities.

Keywords: Ventilation, Infiltration, Indoor Air Quality, Ventilation Efficiency.

This work was supported by the Assistant Secretary for Conservation and Renewable Energy, Office of Building and Community Systems, Building Systems Division of the U.S. Department of Energy under Contract No. DE-AC03-76SF00098, and by research grants from Energy Mines and Resources Canada, and the Natural Sciences and Engineering Research Council of Canada.

NOMENCLATURE

A	Air change (Ventilation) rate ACH [h^{-1}]
$\overline{A}$	Time-averaged air change rate ACH [h^{-1}]
A_e	Instantaneous effective ventilation rate ACH [h^{-1}]
A_m	Effective (temporal-) mean ventilation rate ACH [h^{-1}]
C	Instantaneous pollutant volume concentration [-]
$\overline{C}$	Time-averaged volume concentration [-]
ϵ	Instantaneous ventilation efficiency [-]
ϵ_m	Mean-ventilation efficiency (for a period of time) [-]
S	Instantaneous (pollutant) source strength [h]
$\overline{S}$	Time-averaged source strength [m^3/h]
t	Time [h]
τ_e	Instantaneous turn-over time [h]
$\overline{\tau_e}$	Time-averaged turn-over time [h]
Δt	Discrete time step [h]
α	Weighting factor [-]
i	**Subscript:** The discrete value of the variable for the time interval. $(i-1)\Delta t < t < i\Delta t$

INTRODUCTION

The most common technique for ensuring adequate indoor air quality in buildings is to dilute the concentration of indoor pollutants with fresh air, either by natural ventilation through open doors and windows, air infiltration through envelope leakage, or mechanical (fan) ventilation. Infiltration is the principal mechanism that small residential buildings rely on. This infiltrating air that serves to control the concentration of indoor pollutants also represents air that often must be heated or cooled. The mechanisms involved in pollutant dilution are different from those involved in energy loss, because the ventilation-related quantities that characterize the two processes are different.

Our specific objective here is to examine how the average pollutant concentration responds to ventilation rates that vary with time. The time constant imposed by the internal volume of the building prevents variations in ventilation rate from having an immediate effect on pollutant concentration and, therefore, the average indoor pollutant concentration is not linearly related to the average ventilation rate. It is the intent of this study to define and measure average quantities that describe overall ventilation performance, and to relate these to the (ventilation) air change rates that already have been defined for energy-related calculations.

This report develops a set of effective quantities that can relate time-varying ventilation to pollutant exposures. In principle, the time series (ventilation and emission) data contains all the information necessary to predict pollutant concentrations. However, a significant cross-section of those interested in the topic are accustomed to using steady-state ventilation rates and ventilation efficiencies to calculate air quality. The techniques presented herein convert the time series data into simpler quantities that can be so used; and, in many instances, it may be possible to describe the situation with many fewer values than are contained in the raw data.

BACKGROUND

In most small commercial buildings and virtually all residential buildings, unintentional air infiltration or natural ventilation is the dominant mechanism for supplying fresh air. Infiltration is caused by the interaction between the building's leakage characteristics and the external driving forces caused by the weather [1]. On an annual basis, the average weather-driving forces in North America vary by a factor of three [2] and vary considerably more over shorter periods of time. The tightness of the building's envelope, expressed in terms of the effective leakage area per unit of floor area, has been

shown to vary over one order of magnitude [3]. That is, the infiltration process is marked by variability not only from building to building, but also from climate to climate, and hour to hour. Even within a single building, measured infiltration rates have a standard deviation that is typically half the size of the annual mean.

When assessing indoor air quality, the quantity of interest is usually the average exposure (for our purposes, concentration) of a particular pollutant. Although it is possible to measure directly the average concentration of a pollutant in a particular environment, it is more desirable to have a predictive method that allows one to estimate the average concentration of a pollutant under a wide variety of conditions. Such a model requires knowledge of source strengths and removal mechanisms — ventilation being an important one.

Ventilation is also important for those circumstances where peak exposure is the critical quantity. For such circumstances, it is critical to understand the variations in time of both the source strength and the ventilation (or other removal mechanisms). Depending upon the pollutant, it may not be possible to decouple the source and removal mechanisms. For those pollutants where decoupling is possible, however, simple predictive methods can be developed.

When estimating energy loads related to ventilation, the quantity of interest is the energy required to condition the incoming air. In this case, ventilation plays the same role as heat conductance because its product with the inside-outside temperature difference yields the energy loss. Care must be taken when averaging seasonal infiltration energy loads because of the temperature dependence of infiltration. A new statistic [4] has been proposed to account for weather variations, but for the purposes of this study we shall assume that the average ventilation rate is what is needed to calculate the average ventilation load or the HVAC systems.

Physically, infiltration is caused by pressure differences across leakage sites in the building shell. The leakage characteristics lie somewhere between orifice flow (where the flow rate is proportional to the square-root of the pressure), and viscous flow through long channels (where the flow is proportional to the pressure). These are usually measured with a technique known as *fan pressurization* [5]. The actual driving pressures, both weather-related, are temperature difference and wind. A temperature difference between the inside and outside of a structure induces a density difference between those two bodies of air. This *stack effect* results in a static pressure difference that varies linearly with the height along the wall and with the temperature difference. The static pressure differences caused by the wind are proportional to the square of the wind velocity.

There are many models for predicting infiltration. They range in complexity from single-zone methods useful for houses to complex network models common to large commercial or multifamily buildings. The *Air Infiltration Centre* has prepared a comparison of the models currently used in Western Europe and North America [6]. A simple orifice flow model [2] where the envelope is characterized by its equivalent leakage area has been shown to give an adequate prediction of wind- and stack-induced flow rates [7]. Because the present study relies on measured infiltration rates, the results will not require the use of any a-priori model for infiltration.

POLLUTANT CONCENTRATION AND VENTILATION

If ventilation could be assumed to be constant, there would be no need to treat it differently for assessing indoor air quality as opposed to estimating energy loads. Such a case does exist, for example, in large buildings dominated by constant-volume flow-rate mechanical systems, or for very tight houses that employ exhaust fan ventilation.

For the large majority of small buildings, however, ventilation varies seasonally, diurnally, and randomly. Although energy loads are directly proportional to the ventilation rate, the average concentrations of pollutants are not. Simple arithmetic averaging of the ventilation rate may *not* be a good predictor of average concentration levels of pollutants. To determine the best average to use in predicting pollutant concentration, a closer examination of the dilution process is required.

The expression that describes the conservation of pollutants or tracer gasses is the *continuity equation*:

$$\dot{C}(t) + A(t)\,C(t) = S(t) \tag{1}$$

In general, the volume concentration *(C)*, ventilation (or air change) rate *(A)*, and pollutant source strength *(S)*,are all functions of both location and time. Because we are concentrating on temporal aspects of the measurement problem, we have assumed that the space can be treated as a single zone and that the variables are not functions of position. All sources and sinks other than ventilation are included in the source strength term, *S(t)*.

Although both the ventilation and source terms are time-varying, equation (1) can still be solved in closed form for determining pollutant concentration. The solution of

this first-order linear differential equation is obtained by direct inversion:

$$C(t) = \int_{-\infty}^{t} S(t') \, e^{\int_{t}^{t'} A(t'') \, dt''} \, dt' \tag{2}$$

where t' and t'' are dummy integration variables.

Equation (2) allows us to calculate the current concentration from the complete time history of the source strength and air change rate. For most applications, the behavior before the initial time t=0 is unknown, but the concentration at that time is specified. Rewriting the indefinite solution (2) in terms of this known initial condition, $C(0) \equiv C(t=0)$, yields:

$$C(t) = C(0) \, e^{-\int_{0}^{t} A(t') \, dt'} + \int_{0}^{t} S(t') \, e^{\int_{t}^{t'} A(t'') \, dt''} \, dt' \tag{3}$$

where the first term is an initial transient which decays with time, and the second term is the steady-state solution.

Equation (3) is the general solution for the concentration. Assuming that the ventilation rate and source strength are constant, (3) reduces to the familiar problem of a well-mixed tank:

$$C(t) = C(0) \, e^{-At} + \frac{S}{A} \left(1 - e^{-At} \right) \tag{4}$$

where the first term is the initial transient decay and the second term is the charging term, which contains as the first factor the steady-state solutions.

Once enough time has passed from the initial conditions, equilibrium will be reached and the concentration will be equal to its steady-state value:

$$C = \frac{S}{A} \tag{5}$$

Because the instantaneous ventilation rate, A, will generally be highly variable in time, we will usually not be able to use this simple steady-state equation, which is valid only for constant A.

The general equation (3) does not, by itself, allow us to uncouple the ventilation terms from the source terms without making some further approximations. Most pollutant sources fall into one of two types of emission patterns, slowly-varying emission rates or step-wise constant emission rates. The first is common among organic emissions from (building) materials; the second, among intermittent operations (e.g., CO_2 from a stove).

Assuming that the source strength, S, is effectively constant, we can take it out of the integral in (3) and get the following result:

$$C(t) = S(t)\,\tau_e(t) \tag{6}$$

where we have defined the instantaneous turn-over time, τ_e, as follows:

$$\tau_e(t) \equiv \int_{-\infty}^{t} e^{\int_{t}^{t'} A(t'')\,dt''}\,dt' \tag{7}$$

Although this expression assumes that the source strength is constant, no such constraint is placed upon the ventilation rate, nor is it assumed that equilibrium has been reached. The turn-over time is the characteristic time for the pollutant concentration to approach steady state. It has been defined similarly by Sandberg [8] for the study of the mean age of contaminants. If the ventilation rate, A, was constant for $t \geq 0$ and zero for $t \leq 0$, the turn-over time would be equal to the inverse of the air change rate, $\tau_e = A^{-1}$, the system time constant in equation (4).

To estimate an average pollution exposure level, we need to calculate the mean concentration, which can by found by averaging the above expression over some specified length of time, t_o:

$$\overline{C} = \overline{\left(S(t)\,\tau_e(t)\right)} \tag{8}$$

where the overbars indicate the usual time-averaging convention over time period t_o,

$$\overline{C} = \frac{1}{t_o}\int_{0}^{t_o} C(t')\,dt' \tag{9}$$

Since the source is assumed to be uncorrelated (i.e. constant in time), we can take separate time averages of the emission and turn-over times in (6):

$$\overline{C} = \overline{S}\;\overline{\tau_e} \tag{10}$$

Because Equation (10) assumes S and A to be uncorrelated, pollutants such as radon or formaldehyde, whose emission rates can be affected by the ventilation rate, must be excluded from this study. (This prohibition, of course, can be ignored, if it can be determined that for a particular application the source strength is *not* significantly correlated to the ventilation.)

The same procedure can be applied to pollutants emitted in step-wise constant rates if the general expression (3) is expressed as a sum of terms each of which is treated as

above. For example:

$$C(t) = S_0\,\tau_e(0) + \sum_{n=1}^{\infty}\left(S_n - S_{n-1}\right)\tau_e(t)\,e^{\int_0^{t_n} A(t')\,dt'} \tag{11}$$

where each value of the subscript refers to a discontinuity in the source-strength term.

Effective Ventilation Rate

It is now instructive to reconsider the steady-state limit given by (5). Although this equation is *exactly* true only for the special case where the ventilation rate is constant, it has such an appealing form that it would be desirable to use it for the more general case. We do this by defining an instantaneous *effective ventilation rate* that makes it true:

$$A_e(t) \equiv \frac{S(t)}{C(t)} \tag{12}$$

where A_e is the steady-state ventilation rate that would yield the same *instantaneous* concentration, C, as the actual time-varying conditions.

If we compare this expression with the one for the turn-over time in (7), we find a simple relationship between them:

$$A_e(t) = \frac{1}{\tau_e(t)} \tag{13}$$

which only requires that the source strength S be constant. To define an effective ventilation rate for a specified period of time, we can use the relation for the average turn-over time (10) to define the *effective mean ventilation rate*, A_m, for that period:

$$A_m = \frac{1}{\overline{\tau_e}} \tag{14}$$

so that the average concentration is:

$$\overline{C} = \frac{\overline{S}}{A_m} \tag{15}$$

where A_m is the steady-state ventilation rate that would yield the same *average* concentration, $\overline{C}$, as the actual time-varying conditions.

It is important to recognize that the effective mean ventilation rate, A_m, is *not* equal to the time average of the instantaneous effective rates over the same time interval, $\overline{A_e}$.

This difference is clearly shown when we compare Equations (13) and (14), from which:

$$\frac{1}{A_m} = \overline{\left(\frac{1}{A_e(t)}\right)} \tag{16}$$

Because the inverse of an average is generally different from the average of the inverse, it is essential to distinguish between average ventilation, $\bar{A}$, average effective ventilation, $\bar{A}_e$, and the effective mean ventilation, A_m, rates. It is preferable to first calculate the turn-over time, or average turn-over time, and then calculate the related effective ventilation quantities from it; rather than dealing with the instantaneous effective ventilation.

Ventilation Effectiveness

While the effective ventilation rate is sufficient for calculating pollutant concentrations, it is useful to determine the efficiency of ventilation in controlling indoor air quality. In this way, we can define the **instantaneous** *ventilation efficiency* as:

$$\epsilon(t) \equiv \frac{1}{A(t)\,\tau_e(t)} = \frac{A_e(t)}{A(t)} \tag{17}$$

and the *mean-ventilation efficiency* for a period of time as:

$$\epsilon_m \equiv \frac{1}{\bar{A}\,\bar{\tau}_e} = \frac{A_m}{\bar{A}} \tag{18}$$

where $\bar{A}$ represents the usual time average for the air change rate.

It should be kept in mind that the ventilation efficiency, ϵ, represents a *temporal* efficiency and considers only the time variation of the ventilation, not the local inefficiencies associated with the imperfect mixing of contaminants with incoming fresh air. Because the majority of previous studies of ventilation efficiency have concentrated on mechanical ventilation systems, there has been a tendenct to be concerned with steady-state spatial efficiencies and not with temporal efficiencies. Sandberg [9] has established a comprehensive framework for the discussion of spatial efficiencies, and this should be useful in any discussion of total ventilation efficiency — which must combine both temporal and spatial efficiencies. (Sandberg [10] has similarly considered the case for the spatial efficiency in multiple zones.)

Time-Series Data

Because all measured ventilation rate data is collected in discrete form (for this study, hourly averages), a discrete formulation (i.e., a sum rather than an integral) is more appropriate than the integrals in (3) and (7). If each of the quantities used can be represented by a constant value for a discrete time period $(i-1)\Delta t < t < i\,\Delta t$, the continuous solution for the turn-over time in (7) can be rewritten as:

$$\tau_{e,i} = \sum_{j=0}^{\infty} \frac{1}{A_{i-j}} \left(\frac{1}{\alpha_{i-j}} - 1 \right) \prod_{k=0}^{j} \alpha_{i-k} \tag{19}$$

where α_i is defined as:

$$\alpha_i \equiv e^{-A_i \Delta t} \tag{20}$$

Alternately, we can use the initial values to eliminate the history prior to t=0:

$$\tau_{e,i} = \sum_{j=0}^{i} \frac{1}{A_j} \left(\frac{1}{\alpha_j} - 1 \right) \prod_{k=j}^{i} \alpha_k + \tau_{e,0} \prod_{k=0}^{i} \alpha_k \tag{21}$$

from which the time-averaged turn-over time can be calculated by direct arithmetic averaging:

$$\overline{\tau_e} = \frac{1}{N} \sum_{i=1}^{N} \sum_{j=0}^{i} \frac{1}{A_j} \left(\frac{1}{\alpha_j} - 1 \right) \prod_{k=j}^{i} \alpha_k + \tau_{e,0} \prod_{k=0}^{i} \alpha_k \tag{22}$$

Fortunately, a simple recursive relationship exists that allows the current value of the effective turn-over time to be calculated from the value at the previous time step,

$$\tau_{e,i} = \frac{1-\alpha_i}{A_i} + \alpha_i \, \tau_{e,i-1} \tag{23}$$

These expressions describe single-pole, unity-gain, recursive, digital filters of variable cut-off frequency. The variable cut-off frequency arises because the time constant of the filter is the turn-over time, which varies with time as the infiltration rate varies.

The discrete turn-over time can be used to calculate the discrete instantaneous effective ventilation rate, $A_{e,i}$, and ventilation efficiency, ϵ_i, just as in the continuous case:

$$A_{e,i} = \frac{1}{\tau_{e,i}} \tag{24.1}$$

$$\epsilon_i = \frac{A_{e,i}}{A_i} \tag{24.2}$$

FIELD MEASUREMENTS

The sections above derive the difference between effective and actual ventilation, but they cannot give an indication of whether this difference is likely to be significant (i.e., whether the temporal ventilation efficiency is much different from unity). To make this determination requires measured data that is in some sense typical of real buildings. We have taken ventilation data from an unoccupied test house in Edmonton, Alberta, Canada, for the year of 1984 and calculated the various quantities involved. A diagram of the test house is shown in Figure 1.

Table 1 shows calculations of monthly values for the ventilation rate, the effective ventilation rate, and the ventilation efficiency. Each month represents at least 500 hours of active data collection.

Table 1. Monthly ventilation values for 1984

Month	*Ventilation Efficiency,* ϵ_m *[%]*	*Ventilation Rate, A*		*Turn-over Time,* τ_e	
		Mean $[h^{-1}]$	*Standard Deviation [%]*	*Mean [h]*	*Standard Deviation [%]*
January	92	0.36	35	3.0	28
February	89	0.31	46	3.6	25
March	89	0.34	41	3.3	32
April	92	0.29	36	3.8	28
May	84	0.29	51	4.1	38
June	88	0.18	55	6.5	34
July	86	0.17	62	6.8	40
August	80	0.20	62	6.3	51
September	87	0.26	50	4.4	34
October	83	0.32	49	3.8	42
November	93	0.34	40	3.2	21
December	93	0.39	30	2.8	28
Annual	**81**	**0.28**	**54**	**4.4**	**51**

Inspecting the data for trends reveals a seasonal trend toward higher efficiency during the the severe winter months and lower during the mild summer months. The ventilation rate and its standard deviation also have clear seasonal trends, suggesting that a low ventilation rate and/or a high standard deviation of the ventilation rate is indicative of low ventilation efficiency.

To investigate this variation further, we extracted one week of data from the month with the highest ventilation rate and lowest percentage standard deviation (January), and the month with the lowest ventilation rate and highest percentage standard deviation (July). Figure 2 is a plot of the ventilation rate and turn-over time for one week during January, 1984. The average ventilation rate for that week was 0.41 h^{-1}, and the effective turn-over time was 2.7 h. This yielded a ventilation efficiency rate of 91%. Figure 3 is a plot of the instantaneous ventilation efficiency for the same period of time. For comparison, Figure 3 also shows the actual ventilation rate normalized by the average ventilation rate for the week.

Figures 4 and 5 present the July data in the same way. The average ventilation rate for the data in Figure 4 is 0.21 h^{-1}, the average turn-over time is 5.6 h, and the ventilation efficiency for the week is 85%.

To investigate the effect of averaging time on the bias and scatter of the ventilation efficiency, we calculated ventilation efficiency for different periods of time for both January and July. Figures 6 and 7 present the data. The data for selected averaging times is presented in Table 2 below:

Table 2. Ventilation efficiency for various averaging times

Averaging Time	*January*		*July*	
	Mean Efficiency ϵ_m	*Standard Deviation* [%]	*Mean Efficiency* ϵ_m	*Standard Deviation* [%]
1 hour	1.02	12	1.17	48
8 hours	1.00	8	1.08	24
1 day	0.97	5	0.99	12
3 days	0.95	4	0.96	8

The indoor-outdoor temperature difference ΔT shown in Figures 6 and 7 is the average or the absolute value of the difference, which is the appropriate choice to characterize the stack-effect infiltration rate.

Field Test Findings

The most striking difference between the January and July data is the size of the hourly differences between measured and effective ventilation. Although there is some deviation between the two curves in the January data (Figure 2), the deviations in the July data (Figure 4) are much larger. As expected, the effective ventilation rate, A_e, varies more slowly than does the instantaneous measured ventilation rate. In addition to being obvious from the hourly time-series data, this trend can be seen in the data of Table 1. Note that the percentage standard deviation of the turn-over time is always less than the percentage standard deviation of the measured ventilation rate.

In every month of the year the period-averaged ventilation efficiency, ϵ_m, was less than unity. Although this is a general property for times much longer than the turn-over time, Figures 3 and 5 make it clear that there is a large variation in the hourly ventilation efficiency and that ϵ can exceed unity for short intervals.

The high variability of A_e, τ_e, and ϵ in July is a direct result of the higher (percentage) variability in air infiltration rate, A, during this period because summer infiltration is dominated by the rapidly-varying wind speed, U. In contrast, the infiltration rate in the winter is dominated by the slowly varying indoor-outdoor ΔT. This increases the response time lag which, in turn, increases the difference between A_e and A, making τ_e and ϵ more variable.

Figures 6 and 7 demonstrate the effect of using different averaging time periods to calculate ϵ_m. For shorter base periods, the mean-ventilation efficiency is quite variable. In fact, it is greater than unity more often than not. However, as the base period becomes longer the variation gets smaller, and approaches a value less than unity. This is characteristic of the entire period. As is typical of the other quantities, the variation of ϵ_m during July is higher than that of January.

CONCLUSIONS

In this study we have derived a set of quantities, A_e, ϵ_m, etc, which characterize the ventilation process as it relates to indoor air quality. We have also demonstrated that the fundamental quantity that characterizes this process is the turn-over time, τ_e, and not the ventilation rate, A. Finally, these two quantities can be combined to produce the temporal ventilation efficiency — a key quantity for those concerned with the performance of ventilation systems.

Our derivation clearly distinguishes those quantities that are relevant to indoor air quality from those that are relevant to energy consumption. However, this alone cannot predict the magnitude of the difference between the two. These conclusions are based on our long-term data from a highly instrumented test house and can be generalized qualitatively to other buildings experiencing time-varying ventilation.

The behavior of the ventilation efficiency — the best indicator of ventilation performance — is strongly dependent on the time scale of interest (compared to the turn-over time). For long periods of time (e.g. weeks, months, etc.) the ventilation efficiency shows relatively little variation, but invariably is less than unity. In our data, for example, the monthly ventilation efficiencies ranged between 0.7 and 1.0, the lower values being typical of the months with a high percentage variability, and the upper values being typical of those with less variability. As can be seen from the long-term data, the ventilation efficiency over a very long time period (e.g., one year) is lower than the average of its somewhat shorter constituents (e.g., months).

For time periods on the order of the turn-over time or shorter, the behavior of ventilation efficiency is quite different. It is highly variable and its variability is correlated with the ventilation rate. When the ventilation rate is increasing, the ventilation efficiency is high and may be considerably greater than unity. Conversely, when the ventilation rate is falling the ventilation efficiency may only be a fraction of unity. The lower the ventilation rate, the more exaggerated this effect becomes. Thus, mild periods will experience large swings in ventilation efficiency while extreme periods will be more stable. Although the instantaneous efficiency is quite variable, it is important to note that the *peak* calculated pollutant exposure will never be higher than if one used a ventilation efficiency of unity. This effect is due to the fact that low efficiencies occur during falling, and therefore high, ventilation rates.

The question of what time scale is appropriate is a function of the application. Specifically, it is a function of the operation and occupancy schedule, the type of pollutant, and how that pollutant affects the occupants. If, for example, one is considering a pollutant for which only the accumulated exposure is relevant, then the long term

ventilation efficiency would be appropriate. If, on the other hand, one is considering a pollutant for which the peak exposure value is relevant, then instantaneous values are appropriate. An extreme-value analysis of the effective ventilation rate is a powerful tool for peak-exposure applications.

In presenting these experimental results we have assumed a sufficiently constant pollutant source. That is, we are limiting our conclusions to situations in which the emission is neither highly variable nor correlated with the ventilation. Although this is a reasonable assumption for a wide variety of pollutants; i.e., pollutants whose emission rates are thought to be significantly correlated with the ventilation rate; our assumption of constant source strength is invalid. For example, the estimation of the concentration of Radon emitted from the soil should not be attempted using our technique due to the coupling of the emission with the ventilation. Such questions of variable sources and sources correlated with the ventilation rate require further investigation and are obvious areas for future effort.

Our model represents a powerful tool for the calculation of time-varying pollutant concentrations. The usefulness of this approach will be enhanced when it is combined with those treatments of ventilation efficiency focusing on spatial variations. In the same way that building specification and energy models can be combined with weather data to generate the energy performance indicators, building specifications and this model can be combined with weather data to generate air quality indicators. Efforts are currently under way to investigate such applications.

APPENDIX: DESCRIPTION OF TEST DATA

The Alberta Home Heating Research Facility consists of six unoccupied test houses which have been continuously monitored since 1981 for building envelope energy losses and air infiltration rates. The units allow side-by-side testing to reduce the effects of weather variability when assessing different energy conservation and ventilation strategies.

The test houses are located on the University of Alberta Agricultural Research Farm, approximately 10 km south of the city of Edmonton at 53.5°N latitude. They are situated in a closely spaced, east-west line with about 2.8-m separation between their side walls. False end walls with a height of 3.0-m, but without roof gable peaks, were constructed beside the end houses of the line to provide them with equivalent wind shelter and solar shading.

For purposes of our field tests, we used infiltration data that had been taken during the fall, winter, and summer seasons in test house 5, located colinearly with one house on its east side and a row of four houses to the west.

The flat exposed site is surrounded by rural farmland, whose fields are planted for forage and cereal crops in summer and become snow-covered stubble in winter. Windbreaks of deciduous trees cross the landscape at intervals of a few kilometers, with one such windbreak located approximately 250m to the north of the line of houses. The houses are totally exposed to south and east winds, with a few single-story farm buildings located approximately 50m to 100m to the west, providing some shelter from west to northwest winds.

The wind shelter provided by adjacent buildings was found to be negligible [10], most likely due to an unsheltered flue pipe extending to the level of the roof ridge which acts as a major exfiltration site. In addition, because wind speed is measured directly at a point adjacent to the houses, the effect of varying upwind terrain is accounted for in the wind-speed data. For these reasons, the results of the present study are independent of wind direction and dependent only upon wind speed and indoor-outdoor temperature difference.

Micrometeorological towers are located midway along the row of houses on both the north and south sides of the house line. The wind speed at a 10-m height is measured with low friction cup anemometers and vanes on both towers, with the data-acquisition system recording the value from the tower upwind of the houses. During our tests, there was little variation in the 10-m windspeeds, and the two-tower system simply provided an additional measure of reliability.

The six test units are one-room single-story modules built to residential wood-frame construction standards. Table A1 presents dimensions and infiltration characteristics of test house 5. The floor is about half the size of a typical bungalow, with a floor plan approximately the size and shape of a two-car garage. The 2"x4" stud wall frames rest on full poured-concrete basements. Gable roofs on elevated roof trusses allow for varying levels of attic insulation. The exterior walls of the building are sheathed plywood stained a dark brown. The interior walls are painted drywall over a 4-mil (0.1-mm) polyethylene air-vapor barrier. The locations of the major leakage sites are shown in the Figure 1 schematic (For clarity, the overhanging roof eaves are not shown on the figure.) The air-vapor barrier is penetrated by eight electrical outlet boxes on the inside walls, and three electrical boxes in the ceiling.

Table A1. Dimensions and leakage characteristics of test house #5

Wall perimeter	29m
Wall height	2.4m
Basement height	2.6m
Doorway area	$1.8m^2$
Floor area	$46m^2$
Envelope area	$175m^2$
$\frac{\text{Window area}}{\text{Plan area}}$	0.1
Air volume	$220m^3$

To simulate operation of a forced-air furnace, an electrical heater with ducts is located in the basement. A centrifugal fan distributes air through under-floor ducts. To promote mixing and prevent stratification, air intakes are located near the basement ceiling and floor. The heated air is discharged to the single upper room registers and returns to the basement intake through a large open stairwell. The fan is operated continuously, and inside temperature is controlled with a standard room thermostat set to a constant value of about $22^{\circ}C$. There are no intentional ventilation openings or systems.

Five of the six units, including the one discussed in the present study, have a standard 0.15m I.D. natural gas furnace flue which acts as the major exfiltration site. This unheated flue begins about 1.5m above the basement floor and passes through the upper-level floor, ceiling, and roof to terminate in a rain cap above the roof ridge. Because the unheated flue is continuously filled with room-temperature air, it is equivalent to a leakage site with the same flow resistance located at a height above the ceiling equal to the distance from the ceiling to the rain cap.

Infiltration Measurements

Infiltration measurements were carried out continuously in the six test houses using a constant concentration SF_6 tracer gas injection system Two independent infrared analyzers sample three houses in sequence through a manifold controlled by solenoid valves, as described in [11].

A microcomputer data-acquisition system monitoring the analyzers was used to control the discrete injections of tracer gas required to maintain the concentration at a constant level of 5ppm. The sampling system monitored each of the houses for 2.5 minutes, with a return period of 7.5 minutes to give eight (8) tracer injection pulse counts per hour. This 7.5-minute return period allowed ample time for the previous series of injections to mix completely within the house volume. It also provided the necessary time for the infrared analyzer to draw a sample from an adjacent house. By monitoring and reinjecting tracer gas eight (8) times per hour, the tracer concentration was maintained within 0.2 ppm of the normal 5-ppm setpoint. Each day at 1200 (noon), fresh air was drawn from a line outside the building to check the drift of the infrared SF_6 detectors. Hourly averages of the tracer gas injection rate were recorded along with temperature difference, wind speed, and direction. The measured infiltration rates in m^3/h were divided by the air volume of 220 m^3 to determine the change rate A.

The only significant modifications to the system compared to that described earlier [11,12], were the use of a smaller injector volume to increase injection count resolution, and the automatic zeroing check carried out daily by sampling outside air through a line located on the south meteorological tower. In addition to the daily zero-concentration readings, the detector was calibrated at monthly intervals using a closed-loop system with syringe injection of SF_6 mixtures. (The long-path infrared detector was found to be sufficiently stable to allow monthly calibrations.)

An error analysis of the injection and concentration-measuring systems predicted that the standard deviation in air infiltration flow rate was the sum of $\pm$ 2.5% and $\pm$ 0.5 m^3/h. For the infiltration measurements recorded in unit 5, this represents about a $\pm$ 4% total standard deviation or $\pm$ 8% to encompass 95% of the data.

Whenever a gap of more than one hour occurred in the measurement of infiltration rate, it was necessary to restart the recursive relation (21) used to calculate the effective turnover time in (17). For this restart it was assumed that $\tau_{e,i-1}$ is equal to $\tau_{e,i}$ for the first hour (i.e. when i=1). To avoid the time-lag error associated with this restart procedure, the daily one-hour instrument zero periods were smoothed over by assuming an infiltration rate equal to the average of the preceding and following hourly values.

REFERENCES

1. M.H. Sherman, and D.T. Grimsrud, Measurement of infiltration using fan pressurization and weather data, *Proceedings, 1st AIC Conference, Air Infiltration Instrumentation and Measuring Techniques*, Berkshire, UK (October 1980), Lawrence Berkeley Laboratory Report, LBL-10852.

2. D.T. Grimsrud, M.H. Sherman, and R.C. Sonderegger, Calculating infiltration: implications for a construction quality standard, *Proceedings, ASHRAE/DOE Conference, Thermal Performance of the Exterior Envelopes of Buildings*, Las Vegas, NV (December 1982), Lawrence Berkeley Laboratory Report, LBL-9416.

3. M.H. Sherman, D.J. Wilson, D. Kiel, *Variability in residential air leakage, accepted for publication in Special Technical Publication, ASTM Symposium on Measured Air Leakage Performance of Buildings*, Philadelphia, PA (April 1984), Lawrence Berkeley Laboratory Report, LBL-17587, April 1984.

4. M.H. Sherman, Infiltration degree-days: a statistic for infiltration-related climate, submitted for publication in *ASHRAE Transactions* (June 1986), Lawrence Berkeley Laboratory Report No. LBL-19237.

5. —, Standard Test Method for Determining Air Leakage Rate by Fan Pressurization, *Annual Book of ASTM Standards*, Vol 04.07, E 779, American Society for Testing and Materials, Philadelphia, PA, (1981).

6. M. Liddament, and C. Allen, The validation and comparison of mathematical models of air infiltration, *Technical Note AIC 11*, Air Infiltration Centre, Berkshire, UK (September 1983).

7. M.H. Sherman and M.P. Modera, Comparison of measured and predicted infiltration using the LBL infiltration model, Special Technical Publication of the ASTM Symposium, Measured Air Leakage Performance of Buildings, Philadelphia, PA (April 1984), Lawrence Berkeley Laboratory Report, LBL-17001, February 1984.

8. M. Sandberg and C. Blomqvist, Exploration of ventilation strategies in domestic

housing, *Proceedings, 6th Air Infiltration Centre Conference*, 215.1 (September, 1985).

9. M. Sandberg, M. Sjoberg, The use of moments for assessing air quality in ventilated rooms, *Buildings and Environment* 18, No. 4, 181-195 (1983).

10. M. Sandberg, The multichamber theory reconsidered from the viewpoint of air qualities studies, *Buildings and Environment* 19, No. 4, 221-223 (1984).

11. D.J. Wilson, and J.D. Dale, Measurements of wind shelter effects on air infiltration, *Proceedings, ASHRAE/DOE Conference on Thermal Performance of the Exterior Envelopes of Buildings*, Clearwater Beach, Florida (December 2-5, 1985).

12. D.J. Wilson and W. Pittman, Correlating measured infiltration for wind from a single direction, *ASHRAE Transactions 89*, Part 2B, 211-227 (1983).

FIGURE CAPTIONS

Figure 1: Schematic of test house showing distribution of leakage sites. (Overhanging roof eaves removed for visual clarity.)

Figure 2: January instantaneous measured infiltration rate A and computed effective rate A_e for constant pollutant source strength.

Figure 3: January normalized measured infiltration and computed instantaneous effective ventilation efficiency.

Figure 4: July instantaneous measured infiltration rate A and computed effective rate A_e for constant pollutant source strength.

Figure 5: July normalized measured infiltration and computed instantaneous effective ventilation efficiency.

Figure 6: January ventilation efficiency for varying averaging time periods. Range of measured values shown shaded, with ensemble mean $\bar{E}_{eff}$ shown.

Figure 7: July ventilation efficiency for varying averaging time periods. Range of measured values shown shaded, with ensemble mean $\bar{E}_{eff}$ shown.

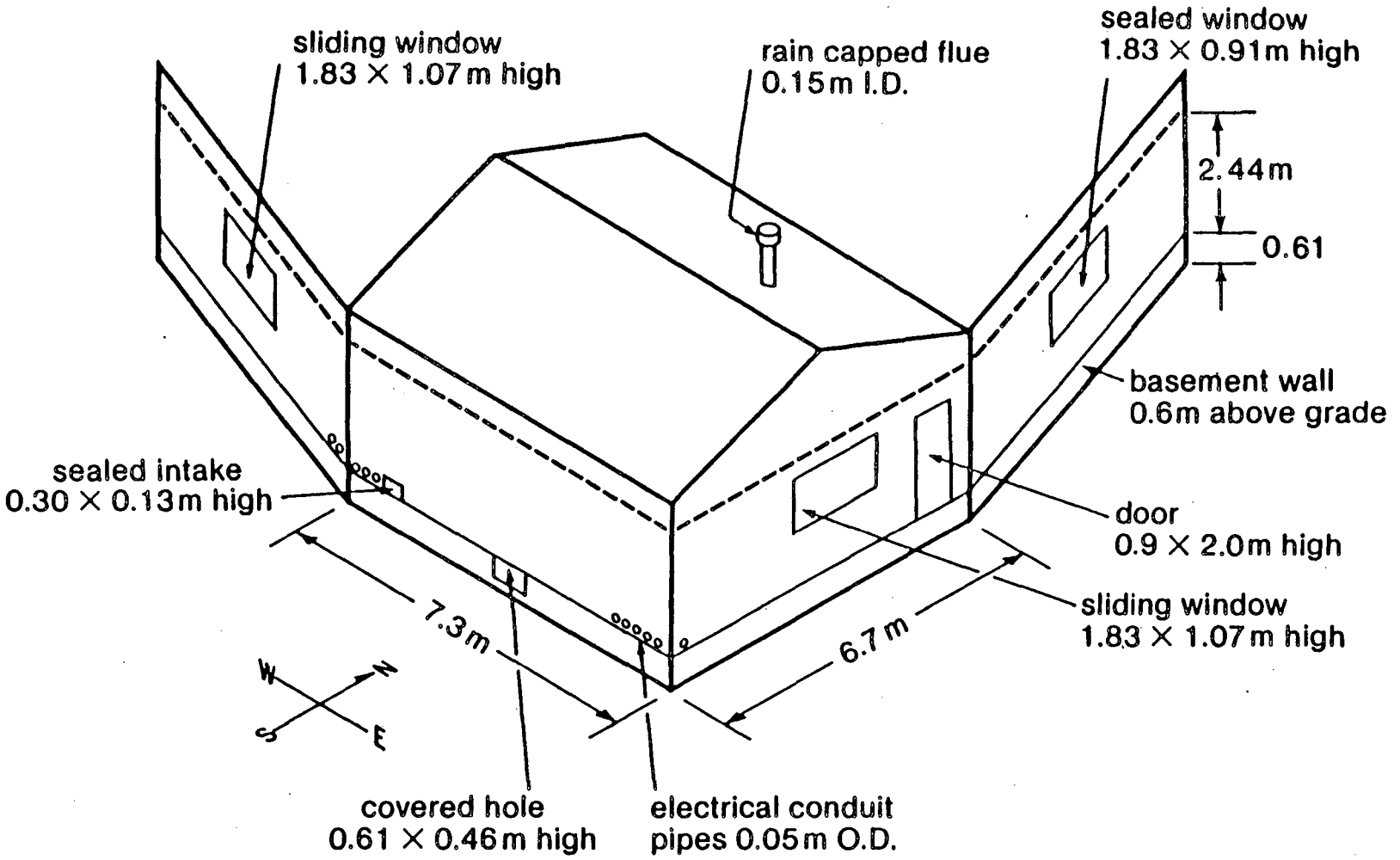

Figure 1: Schematic of test house showing distribution of leakage sites. (Overhanging roof eaves removed for visual clarity.)

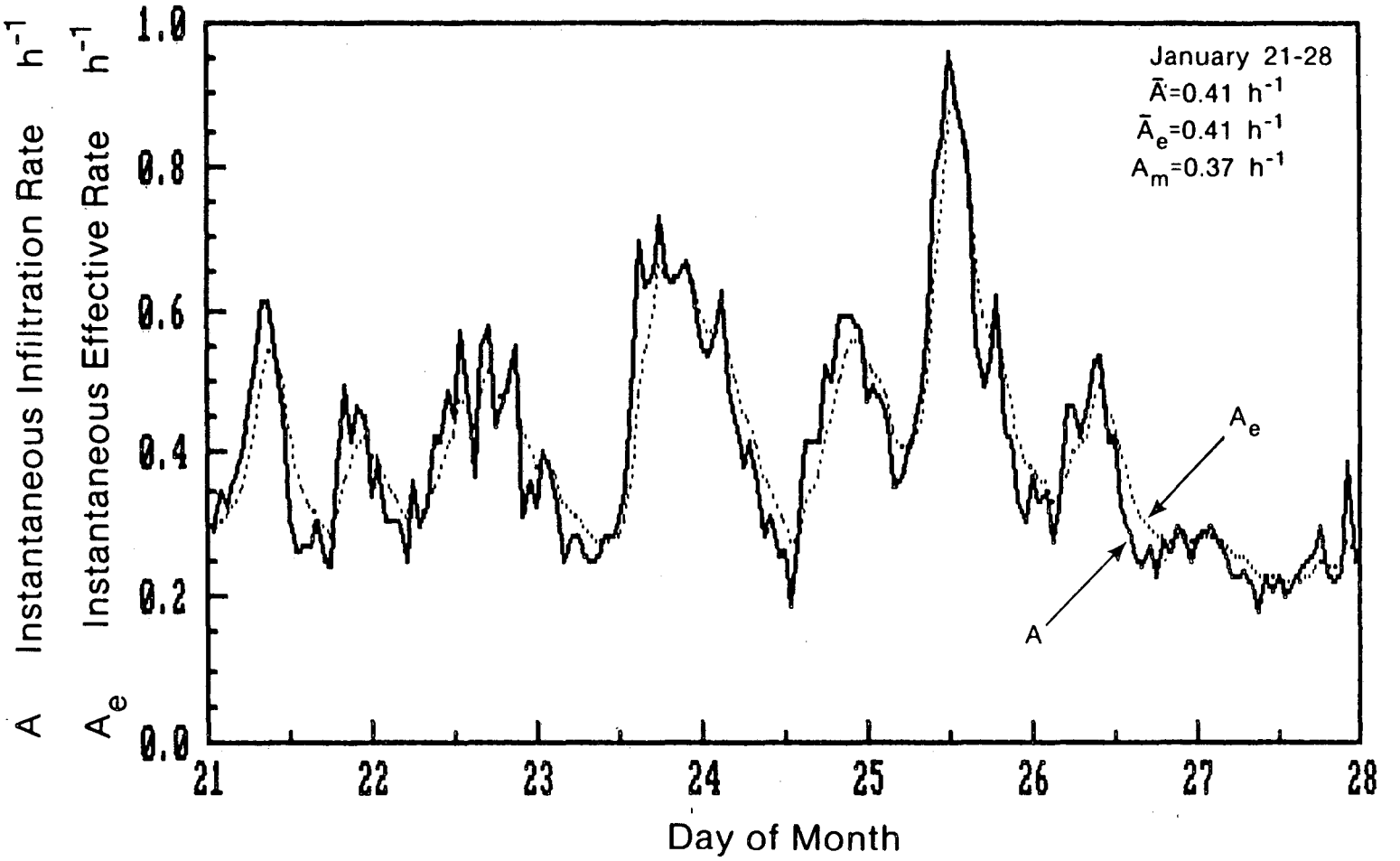

XBL 867-2755

Figure 2: January instantaneous measured infiltration rate A and computed effective rate A_e for constant pollutant source strength.

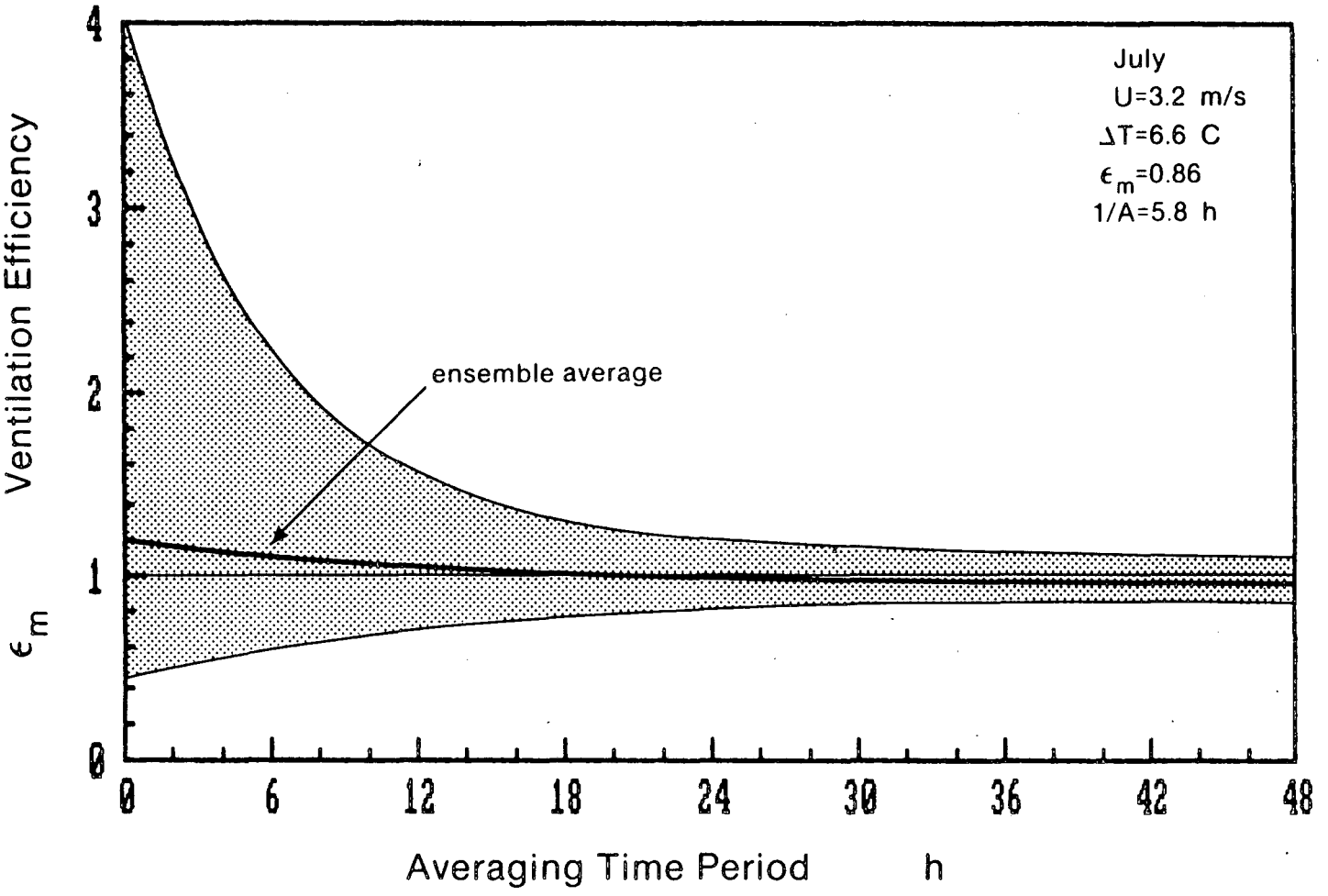

Figure 3: January normalized measured infiltration and computed instantaneous effective ventilation efficiency.

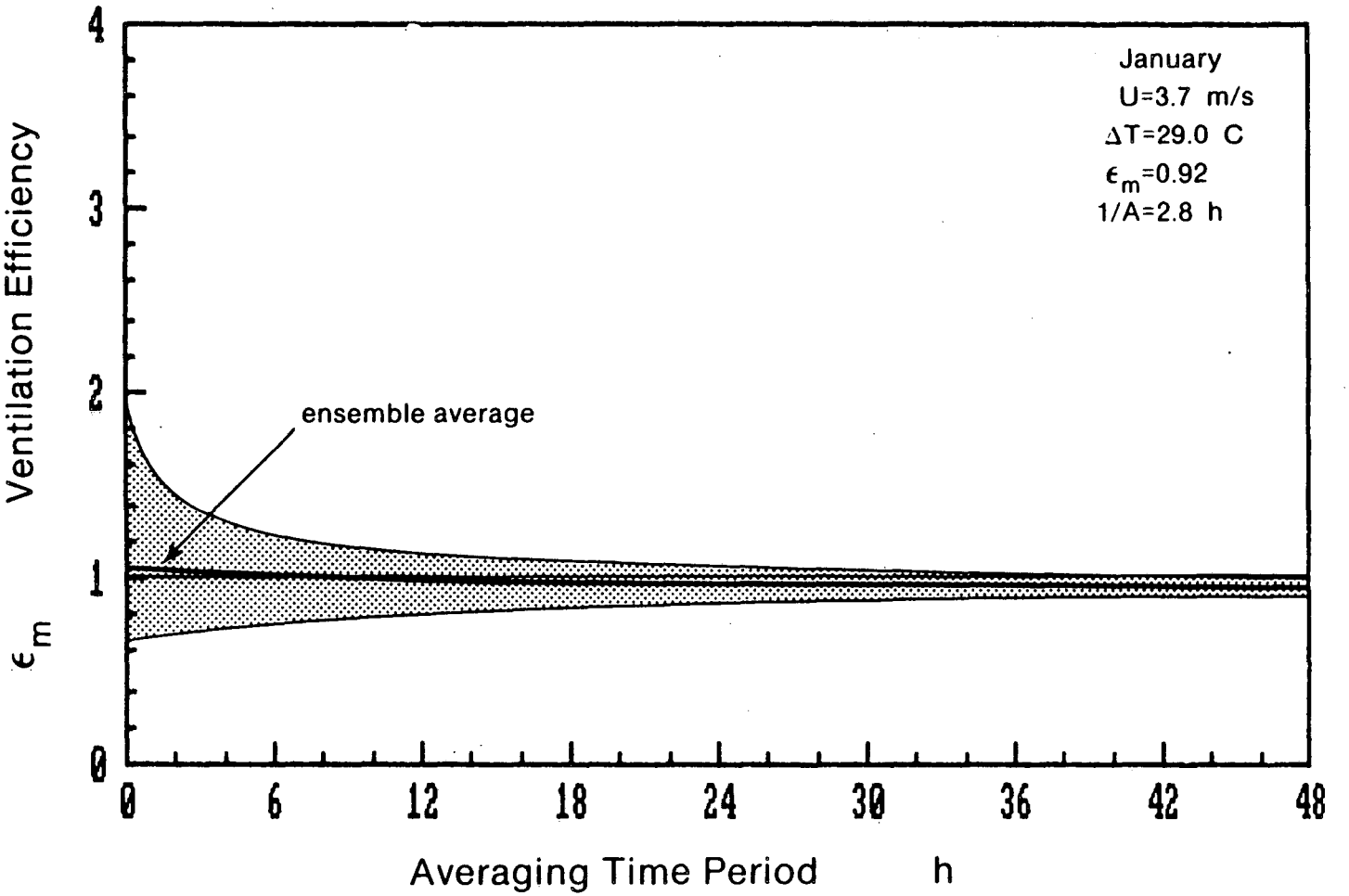

XBL 867-2757

Figure 4: July instantaneous measured infiltration rate A and computed effective rate A_e for constant pollutant source strength.

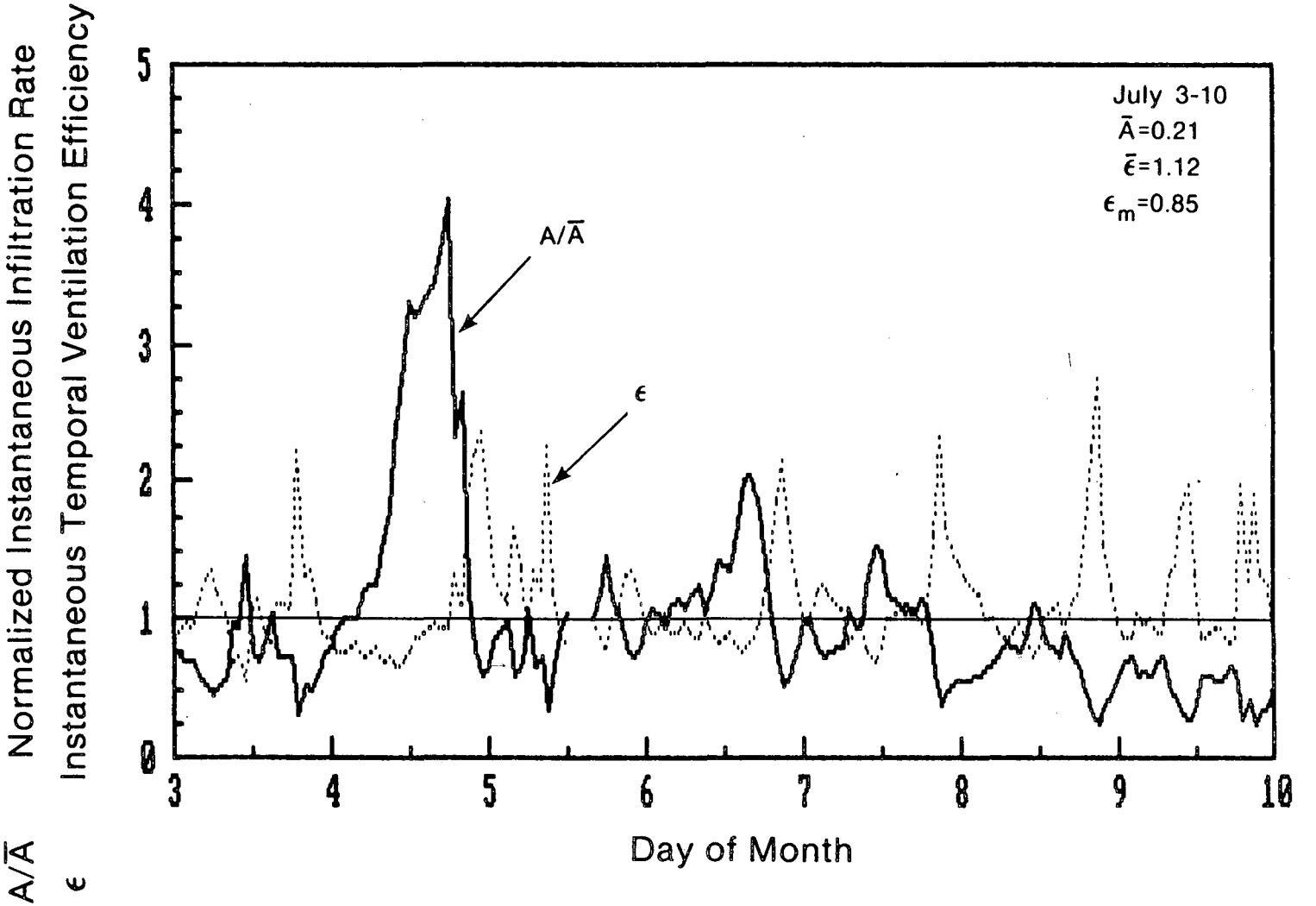

XBL 867-2758

Figure 5: July normalized measured infiltration and computed instantaneous effective ventilation efficiency.

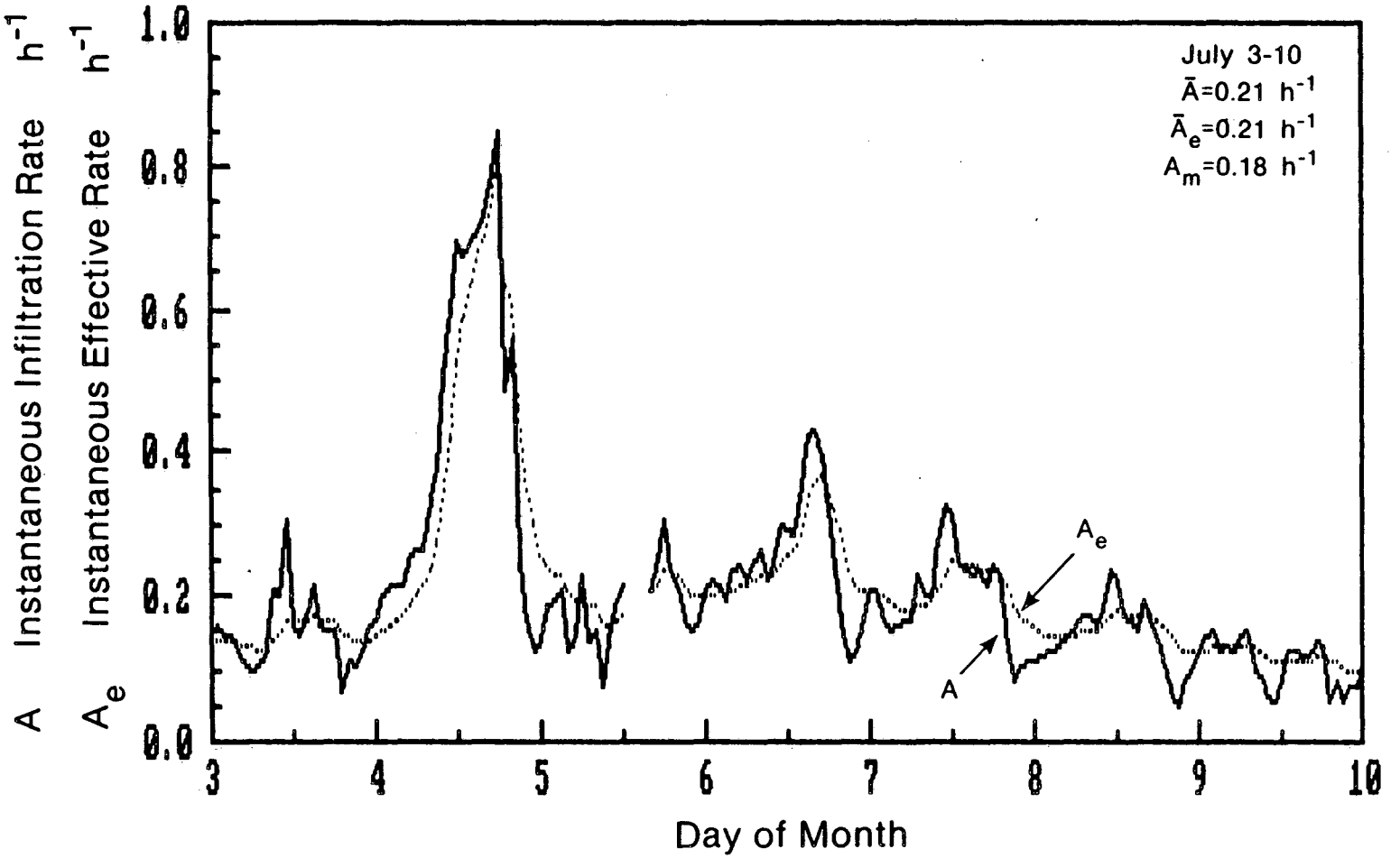

XBL 867-2759

Figure 6: January ventilation efficiency for varying averaging time periods. Range of measured values shown shaded, with ensemble mean $\bar{E}_{eff}$ shown.

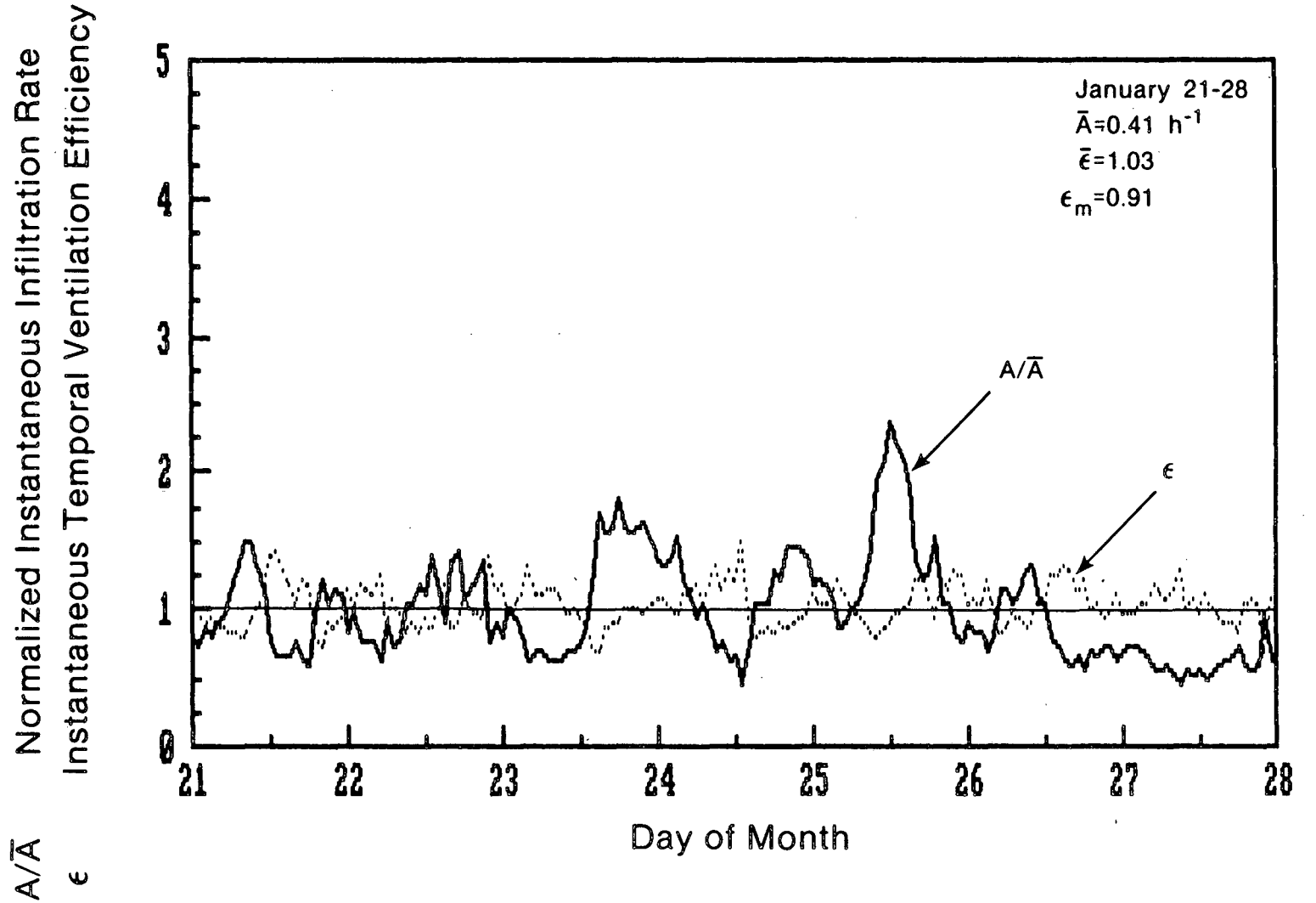

XBL 867-2760

Figure 7: July ventilation efficiency for varying averaging time periods. Range of measured values shown shaded, with ensemble mean $\bar{E}_{eff}$ shown.

LAWRENCE BERKELEY LABORATORY
TECHNICAL INFORMATION DEPARTMENT
UNIVERSITY OF CALIFORNIA
BERKELEY, CALIFORNIA 94720